Illustration of hydrate-based methane gas separation in coal bed methane type gas composition at lower pressures

Burla Sai Kiran, Kandadai Sowjanya, Ch. V. V. Eswari and Pinnelli S. R. Prasad[1,*]

Gas Hydrate Division, CSIR-National Geophysical Research Institute, Hyderabad 500 007, India

Coal bed methane is an emerging and prosperous unconventional energy source, encompassing highly variable (10–70%) mole fractions of methane gas along with other higher hydrocarbon and non-hydrocarbon gases. The gas pressure at the source is typically low, posing technical constraints in the gas separation process. In particular, separation of methane gas from this source is a topic of wider scientific interest. The present study demonstrates the ability of hydrate-based technology in trapping methane gas, in nitrogen (N_2) + methane (CH_4) gas mixture, using tetrahydrofuran (THF)-based hydrate-forming system at lower operating pressures (1.0 MPa). It is observed that the gas trapping is efficient and rapid. All the experiments were conducted at non-stirred condition, which is technically easy to achieve. Mole fraction of CH_4 was increased in proportion with N_2, and it was found that methane gas uptake capacity in hydrate cages, increased progressively with increasing CH_4 concentration. Gas uptake kinetics was also found to be extremely fast and 90% of the gas consumed in hydrates within 50–60 min from hydrate nucleation.

Keywords: Coal bed methane, gas hydrates, lower operating pressure, tetrahydrofuran.

COAL bed methane (CBM) is an unconventional resource for natural gas often associated with coal[1]. The amount of methane buried in the coal mines worldwide is estimated to be of the order of 240×10^{13} m^3, and this rich resource is available in the top 2000 m of the earth's interior[2]. The Indian share is around 18.27×10^9 from degree-III coal mines[3–5]. In India, all underground coal mines are categorized into three degrees depending on emission rates of methane gas. In degrees-I and -II, it is less than 1 m^3/t and 1–10 m^3/t respectively, while degree-III is a gassy mine and methane gas emissions could be higher (>10 m^3/t)[3]. Methane is one of the prominent causes of underground gas explosion accidents in coal mining. It is vital for us to utilize this natural resource passably and properly. Currently, most extracted CBM is mixed with air because of the exploitation technology limitations and reservoir-forming conditions. This CBM has a relatively low content of CH_4, usually ranging from 10 mol% to 45 mol%. However, in order to supply as chemical raw stock or feed gas in the pipeline network of natural gas, CH_4 content in CBM must be higher than 80% (refs 6–8). The potential explosion after mixing CH_4 with air results in tremendous difficulty and risk to process and separate the CBM–air mixture. Consequently, this kind of air-mixed CBM is generally vented to the air directly. Being a greenhouse gas, typically 28 times more effective than CO_2, emission of CH_4 into the atmosphere is of great concern. The global annual discharge of CH_4 from CBM alone is in the range $372–604 \times 10^8$ m^3 (ref. 9). The current focus on CBM is on providing safe mining operations, utilization of methane as an unconventional energy source and mitigate its effect on the environment. In the past this progression of interests provided a vehicle for research, investigations that led to CBM becoming a significant part of the energy resource and a target for exploration and development worldwide[10]. This would augment growing energy needs and lessen the dependency on conventional energy sources. Therefore, research on methods in utilizing air-mixed CBM is highly significant and demanding. It could efficiently mitigate the problem of global warming and utilize natural resources more effectively.

Gas hydrate-based gas separation (GHBS) is one of the most appropriate and attractive approaches to separate CH_4 from air-mixed CBM[11]. Gas hydrates are non-stoichiometric solid compounds, formed by encasing smaller gas (guest) molecules within the polyhedral cages of hydrogen-bonded water (host) molecules, under favourable temperature and pressure conditions[12]. Hydrate separation technology is based on the differences in the composition of the residual gas phase and solid (hydrate) phase after the mixed gas hydrate formation[13,14]. With advantages such as mild experimental conditions, concise technological process, and low energy consumption hydrate separation technology has attracted great attention over the past few decades and has been widely applied to separate various gas mixtures. For example, separation of CO_2 from fuel gas via hydrates formation[14–16]. Since the hydration reactions and subsequent separation processes are conducted in the presence of water, the humid condition can effectively prevent CH_4 from explosion. Thus, hydrate separation technology is suitable to separate CBM–air mixtures[17].

Though the actual air-mixed CBM contains a mixture of CH_4, N_2 and O_2, the O_2 content is far less than CH_4 and N_2 content. Furthermore, the O_2 hydrate formation conditions are close to that of N_2. Thus, practically air-mixed CBM could be treated as a mixture containing only CH_4 and N_2. Estimated formation pressures at 277 K, for CH_4–H_2O (sI) and N_2–H_2O (sII) hydrates are 3.83 and 23.92 MPa respectively[12]. Such high formation pressures for hydrates demand a high level of safety and cost in the experimental set-up and the separation process, restricting

*For correspondence. (e-mail: psrprasad@ngri.res.in)

the extensive application of hydrate separation technology. Therefore, it is necessary to use appropriate hydrate thermodynamics promoter to decrease the formation pressure of CH_4 and N_2 hydrates.

Tetrahydrofuran (THF) is the best among all kinetic and thermodynamic promoters for methane hydrate formation. It can significantly reduce the formation pressure of gas hydrates[18,19]. For example, the formation pressure condition for CH_4 hydrate is 3.83 MPa at 277 K, but in the presence of 6 mol% THF hydrate formation pressure condition is reduced to 0.13 MPa at 277 K. Similarly, for N_2 gas with 5 mol% THF, the hydrate formation condition is reduced to 2.46 MPa at 284.75 K (ref. 20). Also, the hydrate formation is fast (~50–60 min), even under rapid cooling in non-stirred or stirred conditions[21–25]. Therefore, usage of thermodynamic promoters such as THF eliminates the requirement of high-pressure vessels, hence the capital and operational cost for adopting gas hydrate technology for gas separations. The present study deals with hydrate formation in aq-THF with gas mixture, particularly, at lower operating pressures (~1.0 MPa) under non-stirred configuration. Such experiments illustrate the ability of methane gas trapping, in the form of hydrates, using analogous air-mixed CBM gas.

The experimental procedure has been described in an earlier study which was conducted under isochoric conditions[23]. The stoichiometric 5.88 mol% THF was taken to prepare the aqueous solution. The vessel was flushed with feed gas (gas mixture) to remove atmospheric gases. The required amount of nitrogen + methane gas mixture was filled into the experimental vessel to 1.0 MPa at ambient temperature (~298 K). The reactor vessel temperature was rapidly decreased by circulating the cold fluid, since high sub-cooling and driving force play a major role in hydrate crystallization. The *P*–*T* (pressure–temperature) profile was recorded at fixed time-intervals. A sudden pressure drop was observed due to gas consumption in the hydrate cages. Within 1–2 h, 90% of the total consumption occurred. Then, the reactor vessel was warmed up to 300 K to ensure complete hydrate dissociation and recovery of consumed gas. Figure 1 shows the complete process of hydrate formation and dissociation. The process was repeated 2–3 times to ensure the reproducibility and reusability of aqueous THF solutions. The content of gas (mol) in hydrate phase during the experiment at time *t*, is defined by the following equation

$$\Delta nH,\ t = ng,0 - ng,t = (P_0V/Z_0RT_0) - (P_tV/Z_tRT_t), \qquad (1)$$

where *Z* is the compressibility factor calculated by the Peng–Robinson equation of state. The gas volume (*V*) was assumed as constant during the experiments, i.e. the volume changes due to phase transitions were neglected. $ng,0$ and ng,t represent the number of mol of feed (methane) gas at hydrate onset point (zero time) and in the gas phase at any other time *t* respectively. *R* is for universal gas constant and *T* is temperature.

The gas consumption rate was computed using forward differentiation by the following equation

$$\text{Gas uptake rate} = (n_{i+\Delta t} - n_i)/\Delta t, \qquad (2)$$

where Δt is the fixed time interval and n_i is the content of gas at *i*th minute.

The hydrate-forming system consisting of H_2O + THF + CH_4/N_2 crystallizes into sII hydrates with unit cell composition of $16(CH_4/N_2)\cdot8(THF)\cdot136H_2O$. The THF and gas ($CH_4/N_2$) molecules are caged in $5^{12}6^4$ and 5^{12} cages respectively. Figure 2 shows the pressure–temperature trajectory of two extreme gas compositions (i.e.

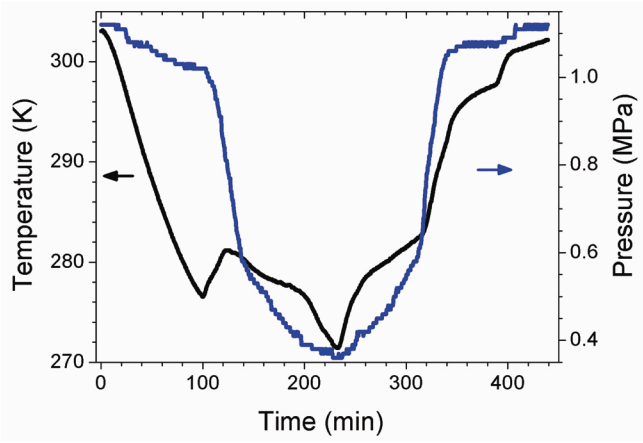

Figure 1. Pressure and temperature variations observed in the hydrate reactor vessel as a function of time. The reactor temperature was decreased/increased rapidly by setting the recirculating chiller bath fluid to –15°C and 25°C. Rapid decrease and increase of reactor pressure respectively, indicates the hydrate formation and dissociation.

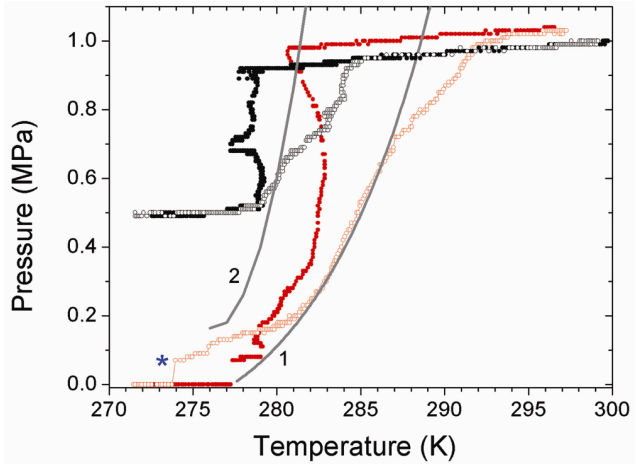

Figure 2. Observed pressure–temperature trajectories for water–THF–N_2 (black)/CH_4 (grey) system. Solid symbols represent the cooling cycle in the hydrate-formation process, while the dissociation behaviour is shown by open symbols. Grey-coloured curves (1 and 2) are the computed phase boundary curves adopted from the literature[18,24] for the H_2O + THF + CH_4/N_2 system. (*) indicates the lower detection limit for the pressure transducer (A10).

Table 1. Observations on the hydrate onset point, gas uptake and rate of gas consumption at different feed gas concentrations

Feed gas		Hydrate onset point		Gas uptake		Rate
X_{CH_4}	X_{N_2}	Temperature (K)	Pressure (MPa)	mmol/mol H_2O	Error	mmol/mol H_2O/min
0	1	278	0.92	3.30	0.57	0.06
0.11	0.89	278	0.89	3.52	0.05	0.11
0.27	0.73	279	0.93	4.86	0.43	0.11
0.38	0.62	279	0.91	5.26	0.18	0.17
0.5	0.5	278	1.03	6.99	0.70	0.17
0.75	0.25	278	0.98	9.02	0.01	0.23
0.89	0.11	280	0.93	9.59	0.32	0.23
1	0	280	0.96	10.34	0.14	0.28

100% N_2 and CH_4) during cooling (formation–filled symbols) and thawing (dissociation–open symbols) cycles at 1.0 MPa. Table 1 shows gas composition in the feed, hydrate onset temperature and pressure, and gas consumption and uptake rate during hydrate formation. It is evident that gas hydrates are formed in both cases and the onset temperature of hydrate formation is ~278 K and ~280 K. In isochroric conditions, the observed pressure drop is proportional to the gas uptake in hydrates and it is relatively less in the system with nitrogen gas. The gas consumption is 3.29 mmol/mol H_2O with 0.09 mol (X_{N_2} = 1.0) of N_2 (feed) gas, while the same with 0.09 mol (X_{CH_4} = 1.0) of CH_4 feed gas is 10.34 mmol/mol H_2O. Interestingly, all these experiments were conducted with identical feed gas pressures and fixed amount of aq-THF solution; and thus there will not be too much variation in the driving force. In fact, the driving force for the CH_4 system at hydrate onset temperature (280 K) is 0.76 MPa. Observed pressure drop upon hydrate formation is maximum in this system and drops to zero, indicating that the residual gas pressure is less than detection limit (0.8 bar) of the transducer (indicate by * in Figure 2). Observed hydrate conversion under such conditions is 2.82% and 8.84% respectively. The hydrate conversion is obtained by dividing gas uptake (mol/mol H_2O) with 0.117 (mol/mol H_2O; the theoretical maximum assuming full 5^{12} cage occupancy in sII system). Such small amounts of hydrate conversion in aq-THF system are not unusual, because the 5^{12} cage-occupancy factor depends on pressure.

All the experiments were conducted with rapid cooling and warming cycles by setting fluid bath temperatures accordingly in order to exploit the potential of gas trapping in aq-THF-based hydrate system. Thus a measurable deviation of dissociation pressure and temperature from ideal phase boundary curve is expected. In fact, as shown in Figure 2, the final dissociation point is shifted to about 3–4 K higher than the phase boundary curve. Usually gas hydrate dissociation experiments are conducted at slow warming (~0.1° h^{-1}). However, we conducted both cooling and thawing cycles at a rapid rate to minimize the process time. We also observed 5–8% increase in gas uptake in experiments conducted at a slower rate. The phase boundary curve, shown as a grey-coloured line in Figure 2, for aq-THF + CH_4 system is adopted from Yoon[26], while that for aq-THF + N_2 system is the extrapolation of literature data points[20]. All the experiments were repeated at least three times to estimate the gas uptake/release due to hydrate formation/dissociation. As shown in Figure 1, the hydrate formation and dissociation is rapid and typically the time required for completion is about 1–1.5 h. Therefore, multi-stage gas separation is possible to effectively trap constituents of CBM gas.

Figure 3 shows the gas uptake in hydrate formed with CH_4 + N_2 gas mixtures. The feed gas composition is systematically varied and we observe at least three times increase in the gas consumption by increasing the CH_4 content in the feed gas mixture. The gas consumption in two extreme cases, i.e. with 100% N_2 (0.09 mol) and 100% CH_4 (0.09 mol) respectively, is 26.68 and 83.69 mmol. With the addition of CH_4 gas, total gas uptake during the hydrate formation process systematically increases from 28.49 mmol (X_{N_2} = 0.9 and X_{CH_4} = 0.1) to 77.56 mmol (X_{N_2} = 0.1 and X_{CH_4} = 0.9). For better comparison, all experiments were conducted with about ~0.09 mol of feed gas resulting in an initial pressure of ~1.0 MPa. Similar experiments have been carried out earlier by Sun *et al.*[27] using CH_4–N_2 gas mixtures with different CH_4 compositions in 6 mol% THF solution in stirred reactor. They also reported an increase in CH_4 fraction in hydrates by increasing CH_4 composition in the feed gas.

Zhao *et al.*[28] have also reported a decrease in the gas separation factor from 9.5451 to 7.1834 upon increasing the reaction pressure from 0.3 to 1.0 MPa in CBM gas mixture consisting of N_2 + O_2 + CH_4 (X_{N_2} = 0.6473, X_{O_2} = 0.1812 and X_{CH_4} = 0.1645). Experimental conditions adopted in the present study are conducive for N_2/CH_4 molecules to occupy vacant 5^{12} cages of sII. Furthermore, our earlier results show that gas uptake, in hydrates passes through a maximum when the amount of aq-THF solution is around 185 ml (ref. 23). Steady increase in gas uptake at higher mole fractions of CH_4

gas indicates that CH_4 is a preferential cage occupant. Therefore, gas uptake increases progressively with CH_4 gas mole fraction.

As already mentioned, we conducted all experiments under non-stirred and isochoric conditions, which are simple and easily adaptable methodologies in large-scale gas separation apparatus. Earlier studies on methane gas separations in CBM under lower pressure (up to 1.3 MPa) used stirred, spray and gas bubbling-type reactors[27–29].

Another important aspect of methane separation is the kinetics of hydrate formation. Figure 4 shows the gas uptake (mmol/mol H_2O) values in the first 2 h duration from onset of hydrate nucleation in various N_2/CH_4 gas mixtures. Figure 5 shows the maximum gas uptake value obtained from forward difference model with 10 min steps using eq. (2). It is evident that maximum gas uptake is in methane-rich systems. The formation rate also shows a systematic increase with increasing CH_4 content in the gas mixture (Figure 5).

As shown Figure 4, gas uptake in hydrates is rather rapid in the first 40–50 min and thereafter, it is slower in gas mixtures. The $t_{90–95\%}$ (time taken for 90%–95% of maximum gas uptake) point in all these cases is only about 75–90 min. Similar formation kinetics has been reported earlier in aq-THF + CH_4 system at moderate pressures[23–25]. Thus, the process is really fast and under such conditions one could consider a sequential gas separation process, namely the gas obtained from hydrate dissociation of first-stage filters could be utilized as feed gas for the next-stage filters. Using such an arrangement, one can easily enrich the methane gas content in CBM gas mixtures.

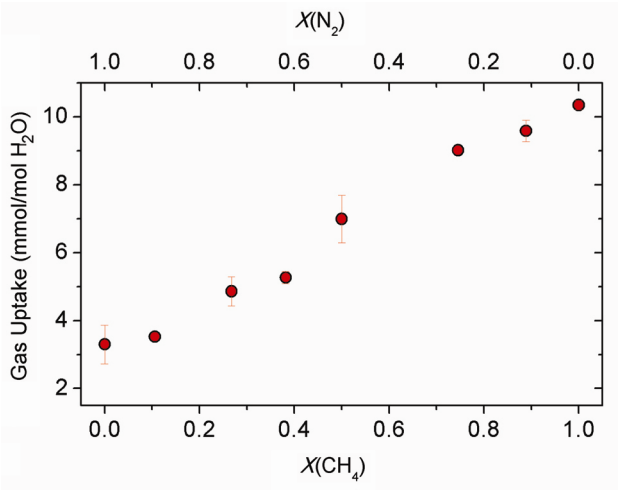

Figure 3. Observed gas uptake values in various gas mixtures of nitrogen and methane. All the experiments were conducted with identical initial gas pressure (1.0 MPa) and 185 ml of aq-THF solution.

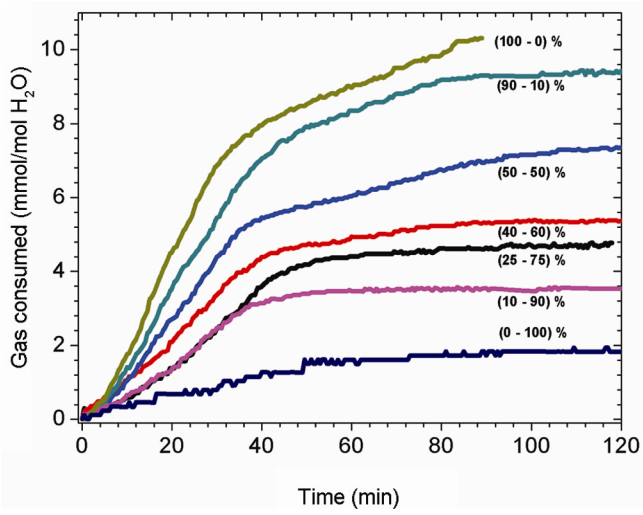

Figure 4. Kinetics of gas uptake in the hydrate formation using CH_4 + N_2 gas mixtures in aq-THF solution. The mole fraction (%) of a gas mixture is shown along each curve.

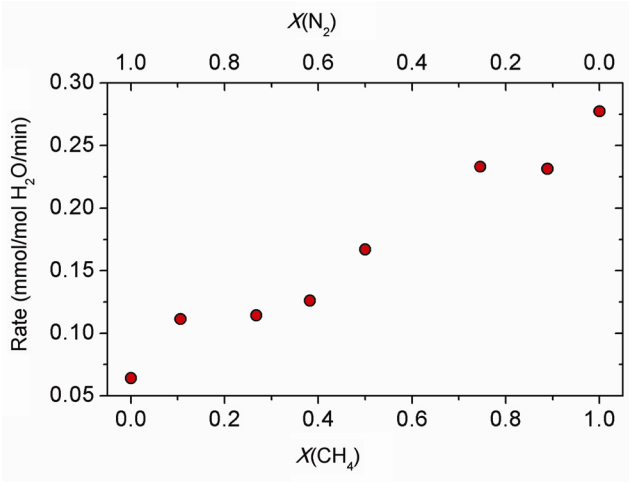

Figure 5. Maximum rate of gas uptake during the hydrate formation process in CH_4 + N_2 gas mixtures.

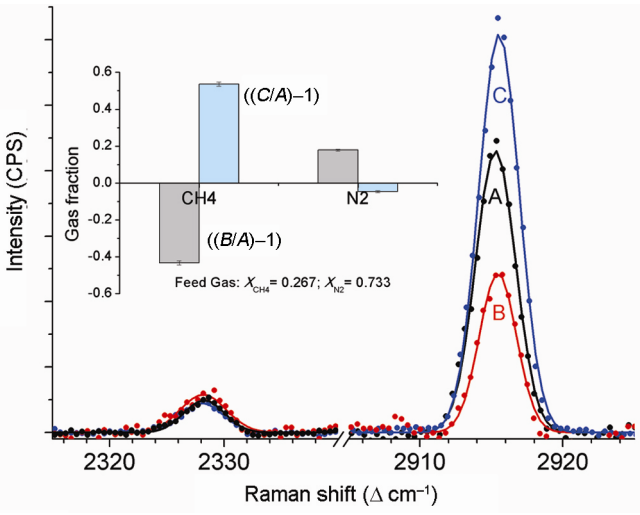

Figure 6. Characteristic Raman band of N_2 and CH_4 gases at various stages, namely in feed (A) and residual (B) gas during hydrate formation process. Also shown are the specific signatures of the gas constituents after hydrate dissociation (C). (Inset) Fraction of CH_4 and N_2 gases at stage B and stage C (see text for details).

Gas chromatography is possibly a direct and easy method for quantification of CBM gas mixtures. Alternatively, we used micro-Raman spectroscopy to probe relative variations (qualitative) in the gas mixtures at various stages of hydrate formation[30]. We obtained Raman signatures of feed gas (before hydrate formation – stage A), the gas equlibration stage (residual gas in vapour phase after hydrate formation – stage B) and finally at stage C after depressurization and hydrate dissociation. Figure 6 shows the Raman signatures obtained for N_2 and CH_4 gas constituents at these stages. Experimental variables like laser power and pressure of the gas cell, etc. were kept constant for all the measurements. The description and peak-fitting procedure is discussed in an earlier study[31]. The resultant histograms shown as inset in Figure 6, represent the gas fraction at each stage. The gas fraction is calculated as the arithmetic difference in peak area at B and A, divided by peak area at A. It is clearly seen from the inset that methane gas content is considerably decreased at stage B and it shows an increment at stage C. On the other hand, opposite signatures are observed for nitrogen gas. These observations corroborate that methane gas is a more preferred guest molecule over for nitrogen in filling vacant 5^{12} cages at lower operating pressures.

In summary, the present study demonstrates the feasibility of utilizing gas hydrate-based separation process to separate methane gas from CBM gas mixtures using stiochemetric aq-THF solution. The experimental conditions utilized, namely non-stirrired and isochoric conditions, operating at 1.0 MPa initial pressure are less technology-demanding and easily adaptable in scale-up process. The main advantage of aq-THF in the hydrate formation could be utilized in designing a gas separation system for air-mixed CBM gas. Such a system will serve the duel purpose of utilizing precious energy, gas and also a considerable reduction in greenhouse gas effect. The present study is a proof-of-concept for showing increased methane molecular trapping in vacant 5^{12} cages of sII over nitrogen molecules in the air-mixed CBM.

1. Bibler, C. J., Marshall, J. S. and Pilcher, R. C., Status of worldwide coal mine methane emissions and use. *Int. J. Coal Geol*., 1998, **35**, 283–310.
2. Liu, C., Zhou, Y., Sun, Y., Su, W. and Zhou, L., Enrichment of coal-bed methane by PSA complemented with CO_2 displacement. *AIChE J.*, 2011, **57**, 645–654.
3. Singh, H. and Mallick, J., Utilization of ventilation air methane in Indian coal mines: prospects and challenges. *Proc. Earth Planet. Sci*., 2015, **11**, 56–62.
4. Singh, A. K. and Kumar, J., Fugitive methane emissions from Indian coal mining and handlingactivities: estimates, mitigation and opportunities for its utilizationto generate clean energy. *Energy Procedia*., 2016, **90**, 336–348.
5. Ojha, K., Mandal, A., Karmakar, B., Pathak, A. K. and Singh, A. K., Studies on the estimation and prospective recovery of coal bed methane from Raniganj coalfield, India. *Energy Sources, Part A*, 2013, **35**, 426–437.
6. Gao, T., Lin, W., Gu, A. and Gu, M., Coalbed methane liquefraction adopting a nitrogen expansion process with propane pre-cooling. *Appl. Energy*, 2010, **87**, 2142–2147.
7. Thakur, P. C., Little, L. G. and Karis, W. G., Coalbed methane recovery and use. *Energy Convers. Manage*., 1996, **37**, 789–794.
8. Chatti, I., Delahaye, A., Fournaison, L. and Petitet, J., Benefits and drawbacks of clathrate hydrates: a review of their areas of interest. *Energy Convers. Manage*., 2005, **46**, 1333–1343.
9. https://www.ipcc.ch/pdf/assessment-report/ar5/syr/AR5_SYR_FINAL_SPM.pdf
10. Flores, R.M., Coalbed methane: from hazard to resource. *Int. J. Coal Geol*., 1998, **35**, 3–26.
11. Babu, P., Linga, P., Kumar, R. and Englezos, P., A review of the hydrate based gas separation (HBGS) process for carbon dioxide pre-combustion capture. *Energy*, 2015, **85**, 261–279.
12. Sloan, E. D. and Koh, C. A., *Clatharate Hydrates of Natural Gases*, CRC Press, Taylor & francis Group, Boca Raton, FL, USA, 2008, 3rd edn.
13. Ma, Q. L., Chen, G. J., Ma, C. F. and Zhang, L. W., Study of vapor–hydrate two-phase equilibria. *Fluid Phase Equilib*., 2008, **265**, 84–93.
14. Kang, S. P. and Lee, H., Recovery of CO_2 from flue gas using gas hydrate: thermodynamic verification through phase equilibrium measurements. *Environ. Sci. Technol*., 2000, **34**, 4397–4400.
15. Seo, Y. T., Moudrakovski, I. L., Ripmeester, J. A., Lee, J. W. and Lee, H., Efficient recovery of CO_2 from flue gas by clathrate hydrate formation in porous silica gels. *Environ. Sci. Technol*., 2005, **39**, 2315–2319.
16. Linga, P., Kumar, R. and Englezos, P., The clathrate hydrate process for post and pre-combustion capture of carbon dioxide. *J. Hazard. Mater*., 2007, **149**, 625–629.
17. Sun, Q., Guo, X. Q., Liu, A. X., Liu, B., Huo, Y. S. and Chen, G. Y., Experimental study on the separation of CH_4 and N_2 via hydrate formation in TBAB solution. *Ind. Eng. Chem. Res*., 2011, **50**, 2284–2288.
18. Chari, V. D., Sharma, D. V. S. G. K. and Prasad, P. S. R., Methane hydrate phase stability with lower mole fractions of tetrahydro-furan (THF) and *tert*-butylamine (*t*-$BuNH_2$). *Fluid Phase Equilib*., 2011, **315**, 126–130.
19. Dong, Q., Su, W., Liu, X., Liu, J. and Sun, Y., Separation of the N_2/CH_4 mixture through hydrate formation in ordered mesoporous carbon. *Adsorp. Sci. Technol*., 2014, **32**, 821–832.
20. Seo, Y. T., Kang, S. P. and Lee, H., Experimental determination and thermodynamic modeling of methane and nitrogen hydrates in the presence of THF, propylene oxide, 1,4-dioxane and acetone. *Fluid Phase Equilib*., 2001, **189**, 99–110.
21. Sharma, D. V. S. G. K., Sowjanya, Y., Chari, V. D., Prasad, P. S. R., Methane storage in mixed hydrates with tetrahydrofuran. *Indian J. Chem. Technol*., 2014, **21**, 114–119.
22. Sowjanya, Y. and Prasad, P. S. R., Formation kinetics and phase stability of double hydrates of C_4H_8O and CO_2/CH_4: a comparison with pure systems. *J. Nat. Gas Sci. Eng*., 2014, **18**, 58–63.
23. Kumar, A., Daraboina, N., Kumar, R. and Linga, P., Experimental investigation to elucidate with tetrahydrofuran rapidly promotes methane hydrate formation kinetics: applicable to energy storage. *J. Phys. Chem. C*., 2016, **120**, 29062–29068.
24. Veluswamy, H. P. *et al.*, Rapid methane hydrate formation to develop a cost effective large scale energy storage system. *Chem. Eng. J*., 2016, **290**, 161–173.
25. Veluswamy, H. P., Kumar, S., Kumar, R., Rangsunvigit, P. and Linga, P., Enhanced clathrate hydrate formation kinetics at near ambient temperatures and moderate pressures: application to natural gas storage. *Fuel*, 2016, **182**, 907–919.
26. Yoon, Ji-Ho, A theoritical prediction of cage occupancy and heat of dissociation of THF-CH_4 hydrate. *Korean J. Chem. Eng*., 2012, **29**, 1670–1673.

27. Sun, Q., Guo, X., Liu, A., Dong, J., Liu, B., Zhang, J. and Chen, G., Experiment on the separation of air-mixed coal bed methane in THF solution by hydrate formation. *Energy Fuels*, 2012, **26**, 4507–4513.
28. Zhao, J., Zhao, Y. and Liang, W., Hydrate based gas separation for methane recovery from coal mine gas using tetrahydrofuran. *Energy Technol*., 2016, **4**, 864–869.
29. Cai, J., Xu, C., Xia, Z., Chen, Z. and Li, X., Hydrate based methane separation from coal mine methane gas mixture by bubbling using the scale-up equipment. *Appl. Energy*; http://dx.doi.org/10.1016/j.apenergy.2017.05.010.
30. Seitz, J. C., Pasteris, J. D. and Chou, I., Raman spectroscopic characterization of gas mixtures: I. Quantitative composition and pressure determination of CH_4, N_2 and their mixtures. *Am. J. Sci*., 1993, **293**, 297–321.
31. Chari, V. D., Prasad, P. S. R. and Murthy, S. R., Structural stability of methane hydrates in porous medium: Raman spectroscopic study. *Spectrochim. Acta A*, 2014, **120**, 636–641.

ACKNOWLEDGEMENTS. We thank the Director, National Geophysical Research Institute (NGRI), Hyderabad for encouragement and permission to publish this paper. Partial financial support from DST and DGH-NGHP, New Delhi is acknowledged. This is a contribution to the GEOSCAPE Project of NGRI under the 12th Five-Year Scientific Programme of CSIR, New Delhi.

Received 23 May 2017; revised accepted 14 September 2017

doi: 10.18520/cs/v114/i03/661-666

Identification of bovine viral diarrhoea virus type 2 in cattle bull semen from southern India and its genetic characterization

Niranjan Mishra[1,*], Semmannan Kalaiyarasu[1], K. C. Mallinath[2], Katherukamem Rajukumar[1], Rohit K. Khetan[1], Siddharth Gautam[1], M. D. Venkatesha[2] and S. M. Byregowda[2]

[1]ICAR-National Institute of High Security Animal Diseases, Anand Nagar, Bhopal 462 022, India
[2]Southern Regional Disease Diagnostic Laboratory, Institute of Animal Health and Biologicals, Hebbal, Bengaluru 560 024, India

Although bovine viral diarrhoea virus (BVDV) is prevalent in Indian cattle causing economic losses in cattle farming, its detection in bull semen has not yet been reported. Following passage of raw bull semen (n = 4) on MDBK cells, testing for BVDV was done by antigen ELISA and real-time RT-PCR. BVDV type-2 (BVDV-2) was identified in three samples from southern India by real-time RT-PCR. Genetic typing of the 5′-UTR sequences classified all the three BVDV strains as BVDV-2a subtype. These were found genetically closely related to the strains from USA, but divergent from the BVDV-2a strains from northern India. Phylogenetic analysis of N^{pro} sequences confirmed the findings. The results provide evidence of circulation of BVDV-2a strains in southern India. The detection of BVDV in bull semen from India highlights the importance of mandatory testing of breeding bulls and bull semen for BVDV to minimize the risk of BVDV transmission.

Keywords: Bovine viral diarrhoea, bull semen, genetic characterization, mandatory testing.

BOVINE viral diarrhoea (BVD) is prevalent worldwide and causes substantial economic losses in cattle farming. Bovine viral diarrhoea virus (BVDV), belonging to the genus *Pestivirus* in the family Flaviviridae is the causative agent of BVD. The *Pestivirus* genus consists of four recognized species, bovine viral diarrhoea virus type-1 (BVDV-1), BNDV type-2 (BVDV-2), border disease virus (BDV) and classical swine fever virus (CSFV)[1]. The BVDV genome consists of a single stranded RNA of positive polarity and is about 12.3 kb in length. A single-open reading frame, flanked by 5′- and 3′-untranslated regions (UTRs) is translated first into a polyprotein and is then cleaved into four structural proteins (C, E^{rns}, E1 and E2) and seven to eight non-structural proteins (N^{pro}, p7, NS2-3, NS4A, NS4B, NS5A and NS5B)[2]. Sequence analysis of the 5′-UTR has been commonly used for *Pestivirus* diagnosis and classification[3–5]. Besides, N^{pro} and E2 regions of the genome are useful for detail phylogenetic analysis[3,4].

Direct or sexual contact with persistently infected (PI) cattle is the major mode of BVDV transmission. However, transmission may also occur through acutely infected animals, artificial insemination (AI), contaminated veterinary equipment and biologicals[6]. BVDV infection in bulls may result in acute infection, persistent infection and prolonged testicular infection or persistent testicular infection (PTI)[7,8]. Semen from transiently infected bulls can transmit BVDV infection and virus can be detected up to 28 days in such bulls[7]. In contrast, concentration of BVDV in both raw and extended semen of PI bulls remains high and semen from PI bulls consistently infects susceptible animals[9]. PTI develops following acute BVDV infection where bulls become nonviraemic and seropositive, but BVDV is detected in semen or testicular tissue and extended cryopreserved semen from such bulls can infect seronegative cows through AI[10,11]. Hence, semen should be tested negative for BVDV prior to its distribution for AI.

BVD is prevalent in India, and BVDV-1, BVDV-2 and BVDV-3 have been detected in cattle[5,12,13]. However,

*For correspondence. (e-mail: mishranir@rediffmail.com)